Acta Cryst. (1986). B42, 314-325

The Immanent Chaotization of Crystal Structures and the Resulting Diffuse Scattering. III. Diffuse Scattering in Perovskites with One-Dimensional Movable Objects ('Shifting')

BY F. A. KASSAN-OGLY AND V. E. NAISH

Institute of Metal Physics of the Ural Scientific Centre, ul. S. Kovalevskoi 18 *GSP*-170, *Sverdlovsk, USSR*

(*Received* 6 *March* 1985; *accepted* 10 *February* 1986)

Abstract

This paper is devoted to the calculation of the diffuse-scattering picture and its temperature evolution in cubic perovskites, the loose-packing of which at high temperatures is connected with the existence of one-dimensional movable objects. The freezing of these objects as temperature decreases leads to structural phase transitions in consecutive order to tetragonal, orthorhombic and rhombohedral phases with accompanying vanishing of relplane families of diffuse scattering. Depending on the values for the ionic radii crystals with one, two or three transitions are possible.

Introduction

The present paper immediately follows parts I and II (Kassan-Ogly & Naish, 1986*a*, *b*). A diagram showing the existence and stability of cubic perovskites was constructed based upon ionic radii in paper II. In the present paper we take into consideration only the perovskites from region (I) of that diagram (shifting).

The cubic lattice constant in these ABX_3 perovskites is determined by the contact of A and X ions so that A ions are immobile; an X ion possesses only one degree of freedom in the direction normal to the face in which it is located while B ions have three degrees of freedom in the X octahedral interstice. In Fig. 8 of part II it can be seen that $KNbO_3$, $BaTiO_3$, $PbTiO_3$, $AgNbO_3$, $KTaO_3$, $CsGeCl_3$, $AgTaO_3$ and perhaps some others belong to this type.

By the mono-Laue method and with the help of monochromatic radiation (Mo $K\alpha$) X-ray patterns of single crystals have been obtained by Harada & Honjo (1967) for $BaTiO_3$ and by Comes, Lambert & Guinier (1970) for $KNbO_3$. The presence of three families of diffuse streaks in these patterns appears to be a peculiar feature of these experiments. Moreover, Comes, Lambert & Guinier examined the temperature evolution of diffuse scattering and revealed that as temperature decreased the subsequent vanishing of three families of streaks takes place at the corresponding phase transitions in $KNbO_3$. Fig. 1 shows schematically four temperature series of experimental patterns obtained by Comes, Lambert & Guinier for $KNbO_3$. In this paper a physical model was proposed, on the basis of which many features of the phenomena taking place in $KNbO_3$ and $BaTiO_3$ could be explained. Henceforth we shall call this the Comes-Lambert-Guinier model (CLG model).

Comes–Lambert–Guinier model

In $KNbO_3$ along each of three cubic [001] axes, crossing the centres of cell one can find $\cdots$Nb$\cdots$O$\cdots$Nb$\cdots$O$\cdots$ chains of ions. At low temperatures it is convenient to regard the $KNbO_3$ structure as an array of equidistant subchains $\cdots$O$\cdots$O$\cdots$ and $\cdots$Nb$\cdots$Nb$\cdots$, displaced opposite each other and frozen in such positions. In such a way the characteristic features of $KNbO_3$: the subsequent appearance of tetragonal, orthorhombic and rhombohedral phases, the appearance of ferroelectricity and the subsequent changing of the spontaneous polarization

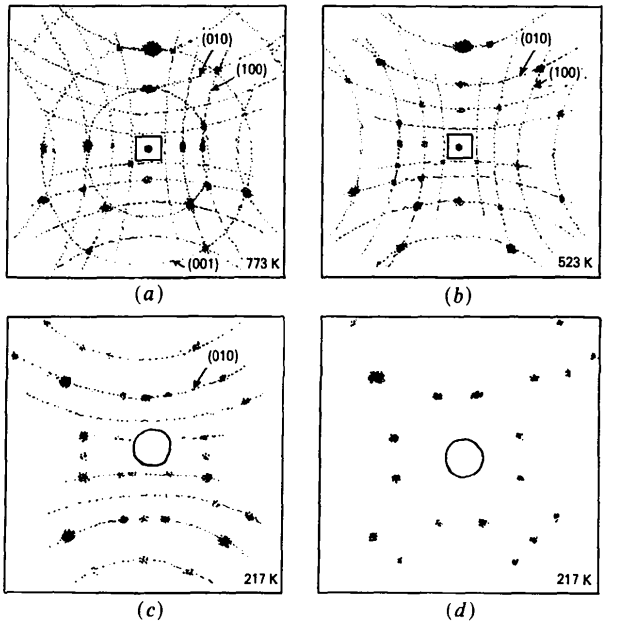

Fig. 1. The scheme of diffuse scattering in $KNbO_3$, observed by Comes, Lambert & Guinier (1970): (*a*) cubic phase, (*b*) tetragonal, (*c*) orthorhombic, (*d*) rhombohedral.

0108-7681/86/040314-12$01.50

direction in structural transitions, could be easily explained. For details we refer the reader to the excellent original paper by Comes, Lambert & Guinier (1970).

In the present paper we use and develop several aspects of the CLG model. First we idealize the rigid subchains assuming them to be *infinite* even at high temperatures and oscillating along their own axes (*parashifting*) owing to the gaps between O and Nb atoms and freezing with increasing displacements (*spontaneous shifting*) as temperature decreases (frozen optical soft phonon). Secondly, we introduce *the interaction parameters* between unidirected chains assuming (owing to cubic symmetry) all J_x, J_y and J_z parameters to be equal. Thirdly, from simple geometric considerations concerning the displacements of all atoms we introduce *the coupling* between the oscillation amplitudes of subchains and the displacements. Fourthly, the chain oscillations in a symmetrical double-well potential (owing to Coulomb instability) are described by the *Ising-model approximation.*

Formulation of the problem

The intensity of the elastic X-ray scattering has the form:

$$I(\varkappa)=\frac{1}{N}\sum_{nn'} f_n f_{n'}^{*} \exp\left[-i\varkappa(\mathbf{R}_n-\mathbf{R}_{n'})\right], \qquad (1)$$

where N is the number of atoms, f_n the X-ray form factor, $\varkappa$ the scattering vector, and $\mathbf{R}_n$ the radius vector of atom n.

In our model each K atom is immobile, each O atom can occupy two positions symmetrical to the cube face, the centre of which is the unstable equilibrium position, and each Nb atom can occupy eight symmetrical positions in the octahedral interstice.

As far as the interaction time of a separate X-ray quantum with a crystal is small compared to the time when the chains change their positions so the scattering intensity would be the average value of the ensemble of elementary scattering acts over all possible crystal configurations.

In the general case, when each movable atom in the crystal may occupy two positions along each of the x, y and z directions, the scattering intensity adopts the form:

$$I(\varkappa)=\frac{1}{LN}\sum_{nn'}\sum_{ll'} f_l f_{l'}^{*} \exp\left[-i\varkappa(\mathbf{R}_{nl}-\mathbf{R}_{n'l'})\right] \times\sum_{\{\sigma\}} p_\sigma \exp\left[-i\varkappa(\Delta_{nl}^{\alpha}\sigma_{nl}^{\alpha}-\Delta_{n'l'}^{\alpha}\sigma_{n'l'}^{\alpha})\right], \qquad (2)$$

where N is the number of unit cells in the crystal, n is the index of a unit cell, L is the number of atoms in a unit cell, l is the index of atom l in a unit cell, and α is x, y, z; $\mathbf{R}_{nl}=\mathbf{R}_n+\mathbf{r}_l$; $\mathbf{r}_l$ is the radius vector of the equilibrium position of ion l in a unit cell; Δ_{nl}^{α} is the displacement vector of the ion with number nl at the oscillation along the α direction; σ_{nl}^{α} is an operator acquiring values $+1$ and -1 at random; p_σ is the statistical weight of a configuration in which each operator has a fixed value; $\sum_{\{\sigma\}}$ is the sum over all configurations of the ensemble.

The unit cell of $KNbO_3$ contains five atoms (see Fig. 2). Let us use the following notations: $f_1=f_2=f_3=f_O$, the oxygen form factor; $f_4=f_{Nb}$, the niobium form factor; $f_5=f_K$, the potassium form factor.

In accordance with our model and the results of paper II Δ_{nl} are equal in every unit cell, *i.e.* they do not depend upon the index n and the vector components are:

$$\Delta_1^x=\Delta_2^y=\Delta_3^z=\Delta_O$$
$$\Delta_4^x=\Delta_4^y=\Delta_4^z=-\Delta_{Nb} \qquad (3)$$
$$\Delta_1^y=\Delta_1^z=\Delta_2^x=\Delta_2^z=\Delta_3^x=\Delta_3^y=\Delta_5^x=\Delta_5^y=\Delta_5^z=0.$$

In $KNbO_3$ three families of chains along the x, y and z directions exist and the subchains oscillate concertedly (rigid subchains) and in antiphase (optical oscillations) so the σ operator does not characterize the positions of separate atoms but of *a chain as a whole.* Moreover the chains oscillate only along their own directions and one obtains: $\sigma_{nl}^x=\sigma_{yz}^x$, $\sigma_{nl}^y=\sigma_{xz}^y$, $\sigma_{nl}^z=\sigma_{xy}^z$, where the subscripts run over all unit cells in the corresponding plane.

As a result, the behaviour of $KNbO_3$ is modelled by the set of three two-dimensional (square) mutually perpendicular Ising lattices with the following Hamiltonian:

$$\mathcal{H}=-\tfrac{1}{2}\sum_{yz;y'z'} 4V^x\sigma_{yz}^x\sigma_{y'z'}^x-\tfrac{1}{2}\sum_{zx;z'x'} 4V^y\sigma_{zx}^y\sigma_{z'x'}^y -\tfrac{1}{2}\sum_{xy;x'y'} 4V^z\sigma_{xy}^z\sigma_{x'y'}^z, \qquad (4)$$

where

$$4V^\alpha = V_{O\text{-}O}^\alpha\Delta_O^\alpha\Delta_O^\alpha+2V_{O\text{-}Nb}^\alpha\Delta_O^\alpha\Delta_{Nb}^\alpha + V_{Nb\text{-}Nb}^\alpha\Delta_{Nb}^\alpha\Delta_{Nb}^\alpha \qquad (5)$$

denotes the interaction between two neighbouring chains parallel to the α axis with coordinates nl and

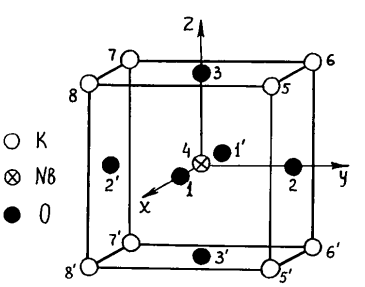

Fig. 2. Numbering of atoms in the perovskite unit cell.

$n'l'$ whereas for cubic symmetry considerations it follows:

$$V^x_{O\text{-}O} = V^y_{O\text{-}O} = V^z_{O\text{-}O}, \quad V^x_{Nb\text{-}Nb} = V^y_{Nb\text{-}Nb} = V^z_{Nb\text{-}Nb}, \quad V^x_{O\text{-}Nb} = V^y_{O\text{-}Nb} = V^z_{O\text{-}Nb}. \tag{6}$$

Hereafter, we shall use the mean-field approximation:

$$\mathcal{H} = -16\sum_{yz} V^x \sigma^x_{yz}\langle\sigma^x\rangle - 16\sum_{zx} V^y \sigma^y_{zx}\langle\sigma^y\rangle - 16\sum_{xy} V^z \sigma^z_{xy}\langle\sigma^z\rangle, \tag{7}$$

where magnitudes $\langle\sigma^\alpha\rangle$ yield the mean-field equation:

$$\langle\sigma^\alpha\rangle = \tanh(J^\alpha\langle\sigma^\alpha\rangle), \qquad \alpha = x, y, z, \tag{8}$$

where the usual notation;

$$J^\alpha = \frac{16V^\alpha}{kT}, \qquad \alpha = x, y, z \tag{9}$$

has been introduced.

The clear physical meaning may be ascribed to the magnitudes $\Delta_{Nb}\langle\sigma^\alpha\rangle$ and $\Delta_O\langle\sigma^\alpha\rangle$, already called (see paper I) *the spontaneous shifting* of niobium and oxygen sublattices.

As a result the scattering intensity adopts the form:

$$I(\varkappa) = \frac{1}{5N}\sum_{nn'}\sum_{ll'} f_l f^*_{l'} \exp[-i\varkappa(\mathbf{R}_{nl} - \mathbf{R}_{n'l'})] \times \sum_{\{\sigma\}} \{\exp[-i\varkappa^x(\Delta^x_l\sigma^x_{yz} - \Delta^x_{l'}\sigma^x_{y'z'}) - i\varkappa^y(\Delta^y_l\sigma^y_{zx} - \Delta^y_{l'}\sigma^y_{z'x'}) - i\varkappa^z(\Delta^z_l\sigma^z_{xy} - \Delta^z_{l'}\sigma^z_{x'y'})] \exp[-\beta\mathcal{H}]\} \times \left\{\sum_{\{\sigma\}} \exp[-\beta\mathcal{H}]\right\}^{-1}. \tag{10}$$

Diffuse-scattering calculation

Let us make use of the mathematical scheme developed in paper I. First, in formula (10) the sum should be taken over the values +1 and −1 of the σ operators. To do this it is convenient to use the calculation contrivance proposed in paper I, namely, under the summation symbol $\sum_{nn'}$ where each index n means the combined indexes x, y and z (coordinates of the unit cell) one has to express unity as a sum of eight terms with the help of Kronecker's δ symbols:

$$1 \equiv (1-\delta_{xx'})(1-\delta_{yy'})(1-\delta_{zz'}) + \delta_{xx'}(1-\delta_{yy'})(1-\delta_{zz'}) + (1-\delta_{xx'})\delta_{yy'}(1-\delta_{zz'}) + (1-\delta_{xx'})(1-\delta_{yy'})\delta_{zz'} + (1-\delta_{xx'})\delta_{yy'}\delta_{zz'} + \delta_{xx'}(1-\delta_{yy'})\delta_{zz'} + \delta_{xx'}\delta_{yy'}(1-\delta_{zz'}) + \delta_{xx'}\delta_{yy'}\delta_{zz'}. \tag{11}$$

Under the summation symbol $\sum_{nn'}$ in the first term one has:

$$\sigma^x_{yz} \neq \sigma^x_{y'z'}, \quad \sigma^y_{zx} \neq \sigma^y_{z'x'}, \quad \sigma^z_{xy} \neq \sigma^z_{x'y'}$$

and, therefore, each sum $\sum_\sigma$ is taken independently. For example,

$$\sum_{\sigma^x_{yz}=+1}^{-1} \exp[-i\varkappa^x\Delta^x_l\sigma^x_{yz} + J^x\langle\sigma^x\rangle\sigma^x_{yz}] = 2\cosh(-i\varkappa^\lambda\Delta^\lambda_l + J^\lambda\langle\sigma^\lambda\rangle) \tag{12}$$

$$\sum_{\sigma^x_{y'z'}=+1}^{-1} \exp[i\varkappa^x\Delta^x_{l'}\sigma^x_{y'z'} + J^x\langle\sigma^x\rangle\sigma^x_{y'z'}] = 2\cosh(i\varkappa^x\Delta^x_{l'} + J^x\langle\sigma^x\rangle). \tag{13}$$

The product of (12) and (13) is $2^2\cosh^2 J^x\langle\sigma^x\rangle\{x\}$, where for the sake of brevity the following notation has been introduced:

$$\{x\} \equiv \cos(\varkappa^x\Delta^x_l)\cos(\varkappa^x\Delta^x_{l'}) + \tanh^2(J^x\langle\sigma^x\rangle)\sin(\varkappa^x\Delta^x_l)\sin(\varkappa^x\Delta^x_{l'}) - i\tanh(J^x\langle\sigma^x\rangle)\sin[\varkappa^x(\Delta^x_l - \Delta^x_{l'})]. \tag{14}$$

Henceforth, in (14) one may substitute $\tanh(J^x\langle\sigma^x\rangle)$ merely by $\langle\sigma^x\rangle$ because of (8).

Beginning with the fifth term in (11) there appear expressions in which some σ operators coincide. Thus, for example, owing to $\delta_{yy'}\delta_{zz'}$ in the fifth term one has $\sigma^x_{yz} = \sigma^x_{y'z'}$ and, as a result, one obtains:

$$\sum_{\sigma^x_{yz}=+1}^{-1} \exp[-i\varkappa^x(\Delta^x_l - \Delta^x_{l'})\sigma^x_{yz} + J^x\langle\sigma^x\rangle\sigma^x_{yz}] = 2\cosh(J^x\langle\sigma^x\rangle)[x], \tag{15}$$

where

$$[x] \equiv \cos[\varkappa^x(\Delta^x_l - \Delta^x_{l'})] - i\langle\sigma^x\rangle\sin[\varkappa^x(\Delta^x_l - \Delta^x_{l'})]. \tag{16}$$

All factors of the $2\cosh(J^x\langle\sigma^x\rangle)$ type are cancelled by the same factors in the denominator of (10).

After the cumbersome calculations the scattering intensity (10) is expressed as a sum of five terms:

$$I(\varkappa) = I_{Br}(\varkappa) + [I^x(\varkappa) + I^y(\varkappa) + I^z(\varkappa)] + I_{bg}(\varkappa). \tag{17}$$

Let us examine the first term:

$$I_{Br}(\varkappa) = \tfrac{1}{5}\sum_{ll'} f_l f^*_{l'} \exp[-i\varkappa\,.\,(\mathbf{r}_l - \mathbf{r}_{l'})]\{x\}\{y\}\{z\} \times \frac{1}{N}\sum_{nn'} \exp[-i\varkappa\,.\,(\mathbf{R}_n - \mathbf{R}_{n'})]. \tag{18}$$

Here $1/N\sum_{nn'}\exp[-i\varkappa\,.\,(\mathbf{R}_n - \mathbf{R}_{n'})] = \sum_{\mathbf{b}}\delta(\varkappa - \mathbf{b})$ is *the intensity of the Bragg reflections* in the reciprocal lattice with vectors $\mathbf{b}$ created by the perovskite simple cubic lattice with parameter a; $\frac{1}{5}\sum_{ll'} f_l f^*_{l'}\exp[-i\varkappa(\mathbf{r}_l - \mathbf{r}_{l'})]$ is the structural factor of perovskite; and $\{x\}\{y\}\{z\}$ is the modulation factor created by the oscillations of chains with amplitudes Δ. The modulation factor is unity in the formal limiting case $\Delta = 0$. At temperatures above the phase transition when

$\langle\sigma^x\rangle=\langle\sigma^y\rangle=\langle\sigma^z\rangle=0$ one obtains:

$$\{x\}\{y\}\{z\}=\cos(\varkappa^x\Delta_l^x)\cos(\varkappa^x\Delta_{l'}^x)\cos(\varkappa^y\Delta_l^y)\times\cos(\varkappa^y\Delta_{l'}^y)\cos(\varkappa^z\Delta_l^z)\cos(\varkappa^z\Delta_{l'}^z),\quad(19)$$

the typical diffuse reducing factor of Bragg reflections (see paper I).

Let us examine the fifth term in (17):

$$\begin{aligned}I_{bg}(\varkappa)=\tfrac{1}{5}|f_{Nb}|^2\{&\sin^2(\varkappa^x\Delta_{Nb}^x)\sin^2(\varkappa^y\Delta_{Nb}^y)\\&\times(1-\langle\sigma^x\rangle^2)(1-\langle\sigma^y\rangle^2)\\&+\sin^2(\varkappa^y\Delta_{Nb}^y)\sin^2(\varkappa^z\Delta_{Nb}^z)\\&\times(1-\langle\sigma^y\rangle^2)(1-\langle\sigma^z\rangle^2)\\&+\sin^2(\varkappa^z\Delta_{Nb}^z)\sin^2(\varkappa^x\Delta_{Nb}^x)\\&\times(1-\langle\sigma^z\rangle^2)(1-\langle\sigma^x\rangle^2)\}.\end{aligned}\quad(20)$$

This expression does not contain δ functions and represents *the diffuse background* continuously distributed over the whole relspace. It is important that it is created only by Nb ions since only Nb ions possess three degrees of freedom. On cooling the background remains because even at the freezing of one of the chain families two degrees of freedom of the Nb ions are left in perpendicular directions. The diffuse background intensity does not depend upon temperature at high temperatures whereas it entirely vanishes in the formal limiting case $\Delta_{Nb}=0$. Owing to the factor of $(1-\langle\sigma^x\rangle^2)$ type it naturally vanishes at $T=0$ ($\langle\sigma^x\rangle=1$).

Three terms of the same kind in (17), $I^x(\varkappa)$, $I^y(\varkappa)$ and $I^z(\varkappa)$, are of most interest to use. Let us examine one of them:

$$\begin{aligned}I^x(\varkappa)=\tfrac{1}{5}\sum_{ll'}f_l f_{l'}^*\exp[-i\varkappa(\mathbf{r}_l-\mathbf{r}_{l'})]\\\times([x]-\{x\})\{y\}\\\times\{z\}\frac{1}{N_x}\sum_{xx'}\exp[-i\varkappa^x(R_x-R_{x'})].\end{aligned}\quad(21)$$

Here the expression

$$\frac{1}{N_x}\sum_{xx'}\exp[-i\varkappa^x(R_x-R_{x'})]=\sum_{b^x}\delta(\varkappa^x-b^x)$$

describes the family of equidistant relplanes normal to the x axis, *i.e. the family of shining diffuse x planes.* The remaining factors in (21) determine the intensity inhomogeneity along these relplanes. Making use of (14) and (16) and the concrete values of $\mathbf{r}_l$ (see Fig. 2):

$$\mathbf{r}_1=\frac{a}{2}(100),\quad\mathbf{r}_2=\frac{a}{2}(010),\quad\mathbf{r}_3=\frac{a}{2}(001),$$

$$\mathbf{r}_4=0,\qquad\mathbf{r}_5=\frac{a}{2}(111),\quad(22)$$

one can reduce (21) to the following form:

$$\begin{aligned}I^x(\varkappa)=\tfrac{1}{5}\{&|f_O|^2\sin^2\varkappa^x\Delta_O^x+|f_{Nb}|^2\sin^2\varkappa^x\Delta_{Nb}^x\\&\times[\cos^2\varkappa^y\Delta_{Nb}^y+\langle\sigma^y\rangle^2\sin^2\varkappa^y\Delta_{Nb}^y]\\&\times[\cos^2\varkappa^z\Delta_{Nb}^z+\langle\sigma^z\rangle^2\sin^2\varkappa^z\Delta_{Nb}^z]\\&-\sin\varkappa^x\Delta_O^x\sin\varkappa^x\Delta_{Nb}^x\\&\times[f_O f_{Nb}^*\exp[-i(\varkappa^x a/2)]\\&\times(\cos\varkappa^y\Delta_{Nb}^y-i\langle\sigma^y\rangle\sin\varkappa^y\Delta_{Nb}^y)\\&\times(\cos\varkappa^z\Delta_{Nb}^z-i\langle\sigma^z\rangle\sin\varkappa^z\Delta_{Nb}^z)+\text{C.C.}]\}\\&\times(1-\langle\sigma^x\rangle^2)\sum_{b^x}\delta(\varkappa^x-b^x).\end{aligned}\quad(23)$$

It is easily seen from (23) that shining diffuse relplanes are created only by Nb and O atoms. The whole diffuse scattering vanishes in the limiting case $\Delta=0$. At temperatures above the phase transition, *i.e.* when $\langle\sigma^\alpha\rangle=0$, the diffuse-scattering intensity is temperature independent.

The behaviour of $I^y(\varkappa)$ and $I^z(\varkappa)$ in (17) in the shape of the y and z relplanes is quite similar to the behaviour of $I^x(\varkappa)$. The families of diffuse relplanes of three orientations reveal themselves in the mono-Laue experiment as corresponding families of streaks on the X-ray pattern (see Fig. 1).

Up to now we have tacitly assumed that temperature dependence is contained only in the J^x, J^y and J^z parameters, the values of which are assumed to be equal. Because, according to the mean-field equations (8), the crystal should undergo a simultaneous phase transition of second order in all three directions and because of the eight equivalent positions for the Nb atom the crystal would be broken into eight types of domains. The crystal structure would be rhombohedral with a simple cubic framework composed of immobile potassium atoms.

In reality the whole picture of the phenomenon is quite different and the real change of the positions of all the ions in the crystal, not just those which participate in shifting, is the physical cause of the phenomenon.

The coupling of spontaneous shifting and structural distortions

Let us assume that in one of the crystal domains as temperature decreases from the parashifting region the phase transition occurs along only one direction, namely along the z axis. This means that the Nb ions have been displaced on average by the value $\Delta_{Nb}\langle\sigma^z\rangle$ along the z axis while oxygen ions 3 and 3′ (see Fig. 2) have been displaced by $\Delta_O\langle\sigma^z\rangle$ opposite to the Nb ion.

As a consequence all four K ions in the upper face (Fig. 2) are drawn nearer because oxygen ion 3 no longer restrains them. Four lower K ions are drawn nearer in the same way. At the same time the four

oxygen ions 1, 1', 2 and 2' in the side faces are also drawn nearer since they are obliged to be on the average at the centres of faces participating in the x and y parashiftings. All these displacements are possible if potassium ions 5 and 5', 6 and 6', 7 and 7', 8 and 8' displace along the z axis. From simple geometrical considerations it is clear that the specific stretch is less than the specific contraction along the x and y axes.

As a result of all these displacements a unit cell and the whole domain is slightly tetragonalized so that the lattice parameters change as follows:

$$a_z = a(1 + l'\langle\sigma^z\rangle)$$
$$a_x = a_y = a(1 - t'\langle\sigma^z\rangle), \qquad (24)$$

where l' and t' are small magnitudes and the new (tetragonal) lattice parameters are denoted a_z, a_x and a_y. Despite all the displacements described above the main condition for perovskite to belong to region I (shifting), namely, the contact between ions A and X, is retained. Fig. 3 shows the change of cell shape at the tetragonalization. This figure shows a cell face normal to the x axis. It is clear that

$$\frac{a}{2}\sqrt{2} = R_A + R_X, \qquad \left(\frac{a_z}{2}\right)^2 + \left(\frac{a_x}{2}\right)^2 = (R_A + R_X)^2.$$

Using (24) one obtains:

$$a_z^2 + a_x^2 = 2a^2,$$
$$a^2(1 + l'\langle\sigma^z\rangle)^2 + a^2(1 - t'\langle\sigma^z\rangle)^2 = 2a^2.$$

Taking into account the fact that in the tetragonal phase $\langle\sigma^z\rangle$ differs little from unity over almost the whole temperature region one obtains a simple approximate relation between l' and t':

$$l' = \sqrt{2 - (1 - t')^2} - 1. \qquad (25)$$

Owing to cubic symmetry it is clear that relations similar to (24) should also exist along the x and y directions. As a result one has:

$$a_x = a(1 + l'\langle\sigma^x\rangle)(1 - t'\langle\sigma^y\rangle)(1 - t'\langle\sigma^z\rangle)$$
$$a_y = a(1 - t'\langle\sigma^x\rangle)(1 + l'\langle\sigma^y\rangle)(1 - t'\langle\sigma^z\rangle) \qquad (26)$$
$$a_z = a(1 - t'\langle\sigma^x\rangle)(1 - t'\langle\sigma^y\rangle)(1 + l'\langle\sigma^z\rangle).$$

The estimation of possible values for the gaps between ions of cubic perovskite, the values of possible displacements at tetragonalization, shows that l' and $t' \sim 10^{-3}$ as in real phase transitions from the cubic to the tetragonal phase in $KNbO_3$, $BaTiO_3$ and so on. Simultaneously with displacements of ions the gaps between them also change and consequently the amplitudes of the sublattice oscillations also have to change:

$$\Delta_{Nb}^x = \Delta_{Nb}(1 + l_{Nb}\langle\sigma^x\rangle)(1 - t_{Nb}\langle\sigma^y\rangle)(1 - t_{Nb}\langle\sigma^z\rangle)$$
$$\Delta_{Nb}^y = \Delta_{Nb}(1 - t_{Nb}\langle\sigma^x\rangle)(1 + l_{Nb}\langle\sigma^y\rangle)(1 - t_{Nb}\langle\sigma^z\rangle) \qquad (27)$$
$$\Delta_{Nb}^z = \Delta_{Nb}(1 - t_{Nb}\langle\sigma^x\rangle)(1 - t_{Nb}\langle\sigma^y\rangle)(1 + l_{Nb}\langle\sigma^z\rangle),$$

where Δ_{Nb} denotes the oscillation amplitude of the Nb subchain in the cubic phase where all $\langle\sigma^\alpha\rangle = 0$. The amplitudes are the same along the x, y and z directions and therefore no longer have the superscript. In general at the appearance of distortions the amplitudes in different directions will be different so that they are denoted by the same symbol Δ_{Nb} but with the superscript.

Quite similar to (27), relations should be written for oxygen amplitudes Δ_O^α in terms of Δ_O.

It should be emphasized that all the parameters Δ_{Nb}, Δ_O, l', t', l_{Nb}, t_{Nb}, l_O, t_O are entirely determined by the ionic radii R_K, R_{Nb}, R_O and by the ratio of the ionic masses M_{Nb} and M_O (K ions are irrelevant for they are immobile in the whole of region I).

The problem of the calculation of these eight parameters turns out to be a complicated independent problem. We shall call it merely *the A problem* and discuss it at length later on. Now attention should be paid to the following simple relation:

$$\frac{\Delta_{NB}}{\Delta_O} = \frac{\Delta_{Nb}^\alpha}{\Delta_O^\alpha} = \frac{M_O}{M_{Nb}} \equiv m; \quad l_{Nb} = l_O \equiv l;$$
$$t_{Nb} = t_O \equiv t. \qquad (28)$$

The first relation merely expresses the mechanics law for optical oscillations; the latter two relations could be easily obtained from (27) and similar formulas for oxygen subchains substituting $\langle\sigma^x\rangle = \langle\sigma^y\rangle = 0$, $\langle\sigma^z\rangle = 1$ and then $\langle\sigma^y\rangle = \langle\sigma^z\rangle = 0$, $\langle\sigma^x\rangle = 1$. It is convenient to rewrite the mean-field equations (8) substituting in them J^α from (9) and $4V^\alpha$ from (5):

$$\langle\sigma^\alpha\rangle = \tanh\left[\frac{4\langle\sigma^\alpha\rangle}{kT}(V_{O\text{-}O}\Delta_O^\alpha\Delta_O^\alpha + 2V_{O\text{-}Nb}\Delta_O^\alpha\Delta_{Nb}^\alpha + V_{Nb\text{-}Nb}\Delta_{Nb}^\alpha\Delta_{Nb}^\alpha)\right].$$

Using the coupling equations (27) and relations (28) one obtains:

$$\langle\sigma^x\rangle = \tanh\left[\frac{4}{kT}(V_{O\text{-}O}\Delta_O^2 + 2V_{O\text{-}Nb}\Delta_O\Delta_{Nb} + V_{Nb\text{-}Nb}\Delta_{Nb}^2)\langle\sigma^x\rangle \times (1 + l\langle\sigma^x\rangle)^2(1 - t\langle\sigma^y\rangle)^2(1 - t\langle\sigma^z\rangle)^2\right].$$

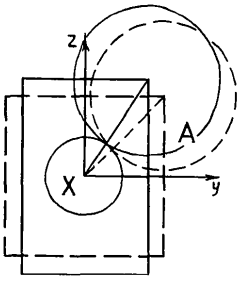

Fig. 3. Perovskite cell distortions (stretch and transverse contraction) at the transition to the tetragonal phase.

Let us introduce the notation:

$$T_0=\frac{4}{k}[V_{O\text{-}O}\Delta_O^2+2V_{O\text{-}Nb}\Delta_O\Delta_{Nb}+V_{Nb\text{-}Nb}\Delta_{Nb}^2]. \quad (29)$$

Finally the mean-field equations will be written as the system of three transcendental equations:

$$\langle\sigma^x\rangle=\tanh\left[\frac{T_0}{T}\langle\sigma^x\rangle \times(1+l\langle\sigma^x\rangle)^2(1-t\langle\sigma^y\rangle)^2(1-t\langle\sigma^z\rangle)^2\right]$$

$$\langle\sigma^y\rangle=\tanh\left[\frac{T_0}{T}\langle\sigma^y\rangle \times(1-t\langle\sigma^x\rangle)^2(1+l\langle\sigma^y\rangle)^2(1-t\langle\sigma^z\rangle)^2\right]$$

$$\langle\sigma^z\rangle=\tanh\left[\frac{T_0}{T}\langle\sigma^z\rangle \times(1-t\langle\sigma^x\rangle)^2(1-t\langle\sigma^y\rangle)^2(1+l\langle\sigma^z\rangle)^2\right]. \quad (30)$$

Thus we have obtained the system for calculating the magnitudes $\langle\sigma^x\rangle$, $\langle\sigma^y\rangle$, $\langle\sigma^z\rangle$ at any temperature T. Any real perovskite from region (I) possesses fixed values of l and t entirely determined by the ionic radii and masses. The temperature of all phase transitions and the temperature dependence of $\langle\sigma^\alpha\rangle$ should be found from solutions of system (30). After that the temperature behaviour of the diffuse intensity could be obtained by formulas (23) as well.

The solution of mean-field equations

At any values of l, t and T_0 the equations (30) yield the zero solution $\langle\sigma^\alpha\rangle=0$. The non-zero solutions may appear in a chosen perovskite only when the temperature reaches that of the corresponding phase transition. If one does not take into account the reconstruction of a lattice, namely, if one puts $l=t=0$, then all the equations become equal:

$$\langle\sigma^\alpha\rangle=\tanh\left[\frac{T_0}{T}\langle\sigma^\alpha\rangle\right].$$

Hence the physical meaning of 'initial' temperature T_0 becomes clear. When the temperature decreases to this value the crystal undergoes a phase transition of second order and the spontaneous shifting begins at this temperature without any lattice distortions whereas $\langle\sigma^x\rangle=\langle\sigma^y\rangle=\langle\sigma^z\rangle$, *i.e.* the freezing of all three families of chains takes place simultaneously so that the new phase appears to be rhombohedral.

However, in reality the spontaneous shifting in one direction immediately involves the corresponding reconstruction of a lattice: ions displace, the shape of the unit cell changes, the gaps between ions partially or completely vanish, the loose packing of the structure decreases, *i.e.* the causes of diffuse scattering under consideration vanish partially or completely. Finally, the conditions for spontaneous shiftings in the other directions change; in particular, the temperatures of the phase transitions change.

It will be shown later on that the temperature T_I of the first phase transition with spontaneous shifting in one direction (for example, along the z direction) differs from T_0, namely, $T_I>T_0$. In contrast, the temperatures of the next phase transitions (if any) with spontaneous shifting along other directions T_{II} and T_{III} are lower than T_0.

In general the system (30) has seven possible types of solutions:

Solution type	σ_1	σ_2	σ_3	Symmetry
0	0	0	0	cubic (trivial)
I	0	0	σ_I	tetragonal
II	0	σ_{II}	σ_{II}	orthorhombic
III	σ_{III}	σ_{III}	σ_{III}	rhombohedral
IV	0	σ_{IV}	σ'_{IV}	low-symmetric
V	σ_V	σ_V	σ'_V	low-symmetric
VI	σ_{VI}	σ'_{VI}	σ''_{VI}	low-symmetric

Here the notations σ_1, σ_2, σ_3 are introduced, each taking the values $\langle\sigma^x\rangle$, $\langle\sigma^y\rangle$ or $\langle\sigma^z\rangle$ depending on the concrete domain.

One should find out the regions of existence of these solutions; then at fixed l and t values the solution with lowest energy should be chosen. The energy formula is obtained by averaging the mean-field Hamiltonian (7) with the help of (5), (9) and (12):

$$E=-16[V_{O\text{-}O}\Delta_O^2+2V_{O\text{-}Nb}\Delta_O\Delta_{Nb}+V_{Nb\text{-}Nb}\Delta_{Nb}^2] \times(A_1^2\sigma_1^2+A_2^2\sigma_2^2+A_3^2\sigma_3^2), \quad (31)$$

where

$$A_1=(1+l\sigma_1)(1-t\sigma_2)(1-t\sigma_3)$$
$$A_2=(1-t\sigma_1)(1+l\sigma_2)(1-t\sigma_3)$$
$$A_3=(1-t\sigma_1)(1-t\sigma_2)(1+l\sigma_3).$$

Hereafter comparing the energies we shall omit the irrelevant constant $16[\cdots]$.

Survey of the solutions

The trivial solution: $\sigma_1=\sigma_2=\sigma_3=0$ exists over the whole temperature region; its energy $E_0=0$.

The tetragonal solution: $\sigma_3=\sigma_I$, $\sigma_1=\sigma_2=0$. In this case the system (30) is reduced to one equation:

$$\sigma_I=\tanh\left[\frac{T_0}{T}\sigma_I(1+l\sigma_I)^2\right]. \quad (32)$$

The tetragonal solution energy is equal to:

$$E_I = -\sigma_I^2(1+l\sigma_I)^2. \quad (33)$$

The orthorhombic solution: $\sigma_1 = 0$, $\sigma_2 = \sigma_3 = \sigma_{II}$. The system (30) is reduced to one equation:

$$\sigma_{II} = \tanh\left[\frac{T_0}{T}\sigma_{II}(1+l\sigma_{II})^2(1-t\sigma_{II})^2\right]. \quad (34)$$

The orthorhombic solution energy:

$$E_{II} = -2\sigma_{II}^2(1+l\sigma_{II})^2(1-t\sigma_{II})^2. \quad (35)$$

The rhombohedral solution: $\sigma_1 = \sigma_2 = \sigma_3 = \sigma_{III}$. The system (30) is reduced to one equation:

$$\sigma_{III} = \tanh\left[\frac{T_0}{T}\sigma_{III}(1+l\sigma_{III})^2(1-t\sigma_{III})^4\right]. \quad (36)$$

The rhombohedral solution energy:

$$E_{III} = -3\sigma_{III}^2(1+l\sigma_{III})^2(1-t\sigma_{III})^4. \quad (37)$$

The simple in principal but rather cumbersome analysis of the equations describing various solutions of the system (30) results in the following conclusions. The tetragonal solution exists from T_I to $T=0$ so that $T_I > T_0$. Both orthorhombic and rhombohedral solutions exist from T_0 to $T=0$. The remaining (low-symmetric) solutions exist in the finite intervals within the interval $(T_0, 0)$. However, the energies of the low-symmetric solutions lie above only one of the symmetric solutions. Therefore, we shall not regard these hereafter. The temperature dependence of σ_I, σ_{II} and σ_{III} is sketched in Fig. 4. The mutual disposition of the curves in this figure does not depend on the numerical values of l and t.

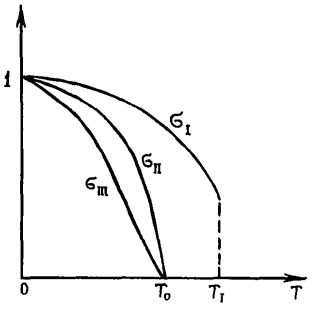

Fig. 4. Temperature dependence of the mean-field equation solutions: σ_I, σ_{II}, σ_{III}.

From the boundaries of the solution existence and from equation (32) one can draw the conclusion that on cooling the crystal initially undergoes a first-order phase transition from cubic to tetragonal. The further temperature behaviour depends upon the numerical values of parameters l and t (more precisely upon t only) determined from the ratios of the ionic radii and masses.

The numerical calculations

The numerical calculations of equations (32)-(37) give four topologically different possibilities for the crossing of different solution energies depending upon the value of the parameter t (see Fig. 5). The solid curve in each figure shows the states of the crystal at different temperatures. Cross-overs on solid curves correspond to the phase-transition points T_I, T_{II} and T_{III}. It should be noted that despite the topological difference of Figs. 5(*b*) and 5(*c*) they both describe one and the same crystal behaviour. Fig. 6 shows the dependence of the phase-transition temperatures upon the t parameter where $t_1 = 1-\sqrt{2/3} \approx 0{\cdot}184$; $t_2 = 1-\sqrt{2}/2 \approx 0{\cdot}293$. The solid curve in Fig. 7 depicts the temperature dependence of the spontaneous shiftings σ_1, σ_2 and σ_3 at various values of t. Thus depending on the t values the perovskite belonging to the 'shifting' region (see diagram in paper II) as temperature decreases are able to undergo one, two or three structural phase transitions in a strict sequence - cubic, tetragonal, orthorhombic and rhombohedral. Fig. 8 shows the results of the numerical calculation of lattice parameters by formulas (26) for crystals with three transitions, *i.e.* for $t < t_1$.

Temperature evolution of diffuse scattering

Let us return to formula (23) for diffuse scattering intensity. Taking into account the relations (27) and (28) and also the unimportant (from a qualitative point of view) simplification $\Delta_O = \Delta_{Nb} \equiv \Delta$ one

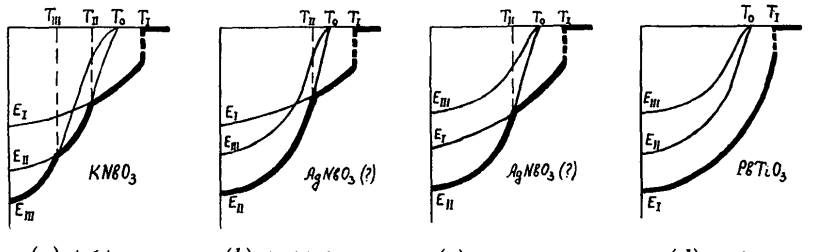

(*a*) $t < t_1$ (*b*) $t_1 < t < t_2$ (*c*) $t_1 < t < t_2$ (*d*) $t_2 < t$

Fig. 5. Temperature dependence of the energies for tetragonal, orthorhombic and rhombohedral solutions. The solid curve indicates the real states of perovskite over the whole temperature region.

obtains:

$$I^x(\varkappa) = (1-\langle\sigma^x\rangle^2)\sin^2[\varkappa^x\Delta(1+l\langle\sigma^x\rangle)(1-t\langle\sigma^y\rangle) \times(1-t\langle\sigma^z\rangle)]M_x(\varkappa)\sum_{b^x}\delta(\varkappa^x-b^x), \quad (38)$$

where the factor $M_x(\varkappa)$ describes the inhomogeneous distribution of intensity along relplanes. Now we shall consider just the common temperature dependence of the intensities of relplanes, that is determined in the main by the first two factors in (38). Let us denote these two factors by $I_x(\varkappa^x)$ and similarly $I_y(\varkappa^y)$ and $I_z(\varkappa^z)$.

$$\begin{aligned} I_x(\varkappa^x) &= (1-\langle\sigma^x\rangle^2)\sin^2[\varkappa^x\Delta(1+l\langle\sigma^x\rangle) \times(1-t\langle\sigma^y\rangle)(1-t\langle\sigma^z\rangle)] \\ I_y(\varkappa^y) &= (1-\langle\sigma^y\rangle^2)\sin^2[\varkappa^y\Delta(1-t\langle\sigma^x\rangle) \times(1+l\langle\sigma^y\rangle)(1-t\langle\sigma^z\rangle)] \quad (39) \\ I_z(\varkappa^z) &= (1-\langle\sigma^z\rangle^2)\sin^2[\varkappa^z\Delta(1-t\langle\sigma^x\rangle) \times(1-t\langle\sigma^y\rangle)(1+l\langle\sigma^z\rangle)]. \end{aligned}$$

Let us consider a typical crystal with three phase temperatures and take, for instance, $t=0{\cdot}125$ and $l=0{\cdot}1$. We shall compare the intensities of equivalent relplanes from three families; for example, the second ones $\varkappa^x=\varkappa^y=\varkappa^z=(2\pi/a)2$. The value of Δ has been taken equal to $0{\cdot}025\ a$. To facilitate comparison with the experiment by Comes, Lambert & Guinier (1970) we shall assume that the first phase transition occurs along the z axis, then along the x axis, and finally along the y axis. Fig. 9 shows the calculated temperature dependence of the diffuse relplane intensities and for the sake of discussion the temperature dependence of the two factors is shown as well. The non-monotonous behaviour of the factor of $\sin^2\varkappa^x\Delta^x$ type should be emphasized since it may give, at some value of the parameters, even an increase of the diffuse scattering intensity with temperature decrease.

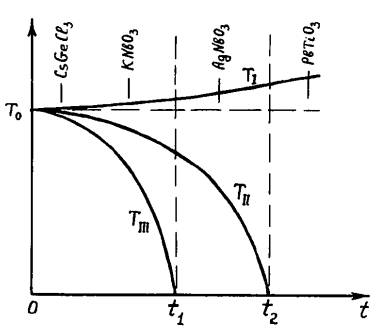

Fig. 6. The dependence of phase-transition temperatures upon the t parameter. $t_1\approx 0{\cdot}184$; $t_2\approx 0{\cdot}293$.

Comparison with experiment

The temperature dependence of diffuse relplane intensities shown in Fig. 9 describes the experimental situation that takes place in $KNbO_3$ and is shown in Fig. 1 of Comes, Lambert & Guinier (1970), whereas $I_y(\varkappa^y)$ in Fig. 9 agrees well with Fig. 7 of their paper.

The calculated behaviour of the lattice parameters shown in Fig. 8 is in good agreement with the experimental data for $KNbO_3$ of Kay & Vousden (1949). Similar pictures can be obtained for crystals with one or two transitions. Figs. 7(a) and 7(c) reproduce with good agreement (with σ redesignated by **P**) the behaviour of spontaneous polarization in the ferroelectrics $KNbO_3$, $BaTiO_3$ and $PbTiO_3$ obtained by Triebwasser (1956), Merz (1949, 1953) and Remeika & Glass (1970) accordingly, including the direction and reorientation of spontaneous polarization **P** at phase transitions. The numbers and types of domains observed in the experiment also agree with our theory.

Let us now compare $KNbO_3$ and $BaTiO_3$, which according to numerous experimental data behave like twins. They both undergo the same cascade of three structural phase transitions with identical crystal structures and so on. However, the diffuse X-ray pattern obtained for $BaTiO_3$ in the cubic phase by Harada & Honjo (1967) differs markedly from the corresponding picture for $KNbO_3$ obtained by Comes, Lambert & Guinier (1970). It is so much weaker that one family of diffuse streaks (circular ones) was not even observed despite the fact that the

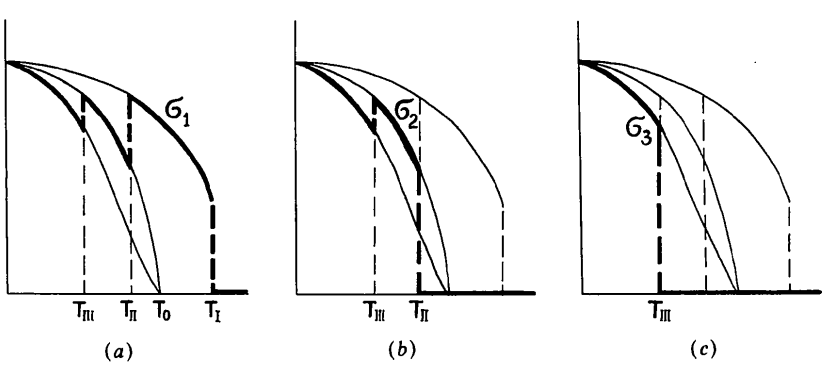

Fig. 7. Temperature dependence of spontaneous shifting in three directions for a crystal with three transitions ($KNbO_3$ type).

exposure time was 120 h for $BaTiO_3$ against 2 h for $KNbO_3$. The first reason which comes to mind is the difference between the niobium and titanium form-factor values since they both exceed that of oxygen and thus niobium and titanium subchains provide the main contribution to the diffuse scattering intensity according to formula (23). But this difference ($f^2_{Nb} \approx 132; f^2_{Ti} \approx 38$) is not enough to explain the much greater experimental difference between $KNbO_3$ and $BaTiO_3$. Luckily we have the other valuable factors in (23), namely, the factors of $\sin^2 \varkappa^x \Delta^x_{Nb}$ type. Here Δ_{Nb} (or Δ_{Ti}) is determined, firstly, by a gap between the Nb ion (Ti ion) and the oxygen ion and, secondly, its share of a gap is determined by relation (28):

$$\frac{\Delta_{Nb}}{\Delta_O} = \frac{M_O}{M_{Nb}} \left(\frac{\Delta_{Ti}}{\Delta_O} = \frac{M_O}{M_{Ti}} \right).$$

The niobium–oxygen gap is greater than the titanium–oxygen gap which is seen in the diagram in paper II since $KNbO_3$ is farther than $BaTiO_3$ from the close-packed point *A*. The relative share of the niobium amplitude is also greater than that for titanium according to (28). These are two additional reasons for the weakness of the diffuse scattering in $BaTiO_3$ compared with $KNbO_3$.

Discussion. Other experimental examples

Thus the mathematical description developed for the loose packing of a crystal structure and the resulting diffuse scattering together with the further development of the Comes–Lambert–Guinier model gives for the first time not only a qualitative but also a detailed quantitative description of the whole phenomenon taking place in shifting perovskites, namely, X-ray pattern tracery, its temperature evolution, the cascade of structural phase transitions, orders of transitions, temperature behaviour of lattice constants, spontaneous polarization and so on.

It should be reiterated that the method of X-ray diffraction of a monochromatic beam on a fixed single crystal (mono-Laue method) appears to be a powerful instrument for structural studies of a crystal with a loose-packed lattice. Unfortunately very few experiments have been carried out with this method up to now.

The lattice loose packing in ionic crystals is caused by the ratios of the ionic radii and owing to gaps between them can lead to the existence of movable one-dimensional (parashifting) or two-dimensional (paratilting) objects. If the oscillations of these objects take place in a multi-well potential (here double-well potential in the Ising approximation) they can freeze as temperature decreases creating, owing to coupling equations (27), structural phase transitions to new phases. In the present paper the investigation of perovskites with movable chains has led to the discovery of the existence of perovskites with either one, two or three transitions in the shifting region (I). For example, all the crystals falling in the region with $t < t_1$ (Fig. 6) possess three phase transitions, like $KNbO_3$ or $BaTiO_3$ in which three transitions were observed experimentally. The crystal $CsGeCl_3$ falls into the same region but in the experiment by Christensen & Rasmussen (1965) only one transition from the cubic structure directly into the rhombohedral one is observed. A possible explanation is that at very small t value $CsGeCl_3$ should possess three transitions with very close phase-transition temperatures T_I, T_{II} and T_{III}, which had not been successfully split in experiment. The $PbTiO_3$

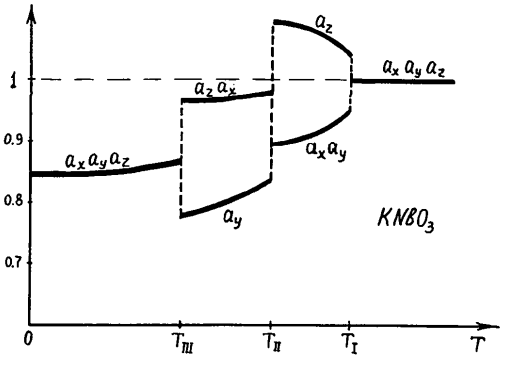

Fig. 8. Calculated temperature dependence of the lattice parameters for a crystal with three transitions ($KNbO_3$ type).

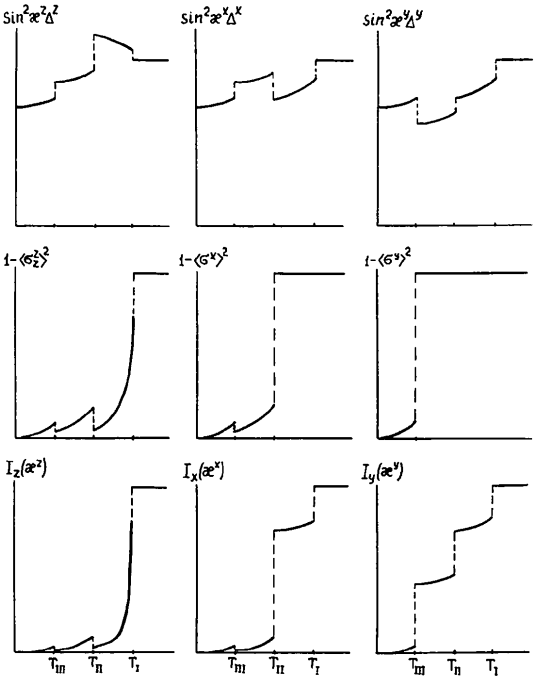

Fig. 9. Calculated temperature dependence of the diffuse-scattering intensity for three families of relplanes (z, x and y) – lower curves. The upper curves describe the two separate factors $(1-\langle\sigma\rangle^2)$ and $\sin^2 \varkappa^\alpha \Delta^\alpha$.

crystal with one phase transition from a cubic to a tetragonal phase observed in experiment apparently corresponds to the $t > t_2$ region in Fig. 6. In the region $t_1 < t < t_2$ one can find two perovskites, $AgNbO_3$ and $AgTaO_3$, with two phase transitions, observed by Francombe & Lewis (1958), from a cubic into a tetragonal and then into an orthorhombic structure. These two crystals are apparently antiferroelectrics, the oscillating chains in them do not freeze in the same order as in $KNbO_3$, but in chess-board order (antishifting) which corresponds to a negative sign for the chain-interaction parameter. Discussion of this question may be found in Alexandrov, Anistratov, Besnosikov & Fedoseeva (1981) or in Lines & Glass (1977). The behaviour of such crystals could be described in our theory with slight change; namely, to describe antishifting one should introduce two sublattices in each direction, as is usually done in the theory of antiferromagnetism.

Certain attention should be paid to $KTaO_3$ in which no transitions had been observed. According to the values of the ionic radii it has to undergo three phase transitions; however, the transition temperatures are determined not only by the t values but also by the chain-interaction parameter J which is only very small and the transition temperatures are also very small. The experimental study of the mixed compounds $KNbO_3$–$KTaO_3$ obtained by Triebwasser (1959) and discussed by Jona & Shirane (1962) gives support to such suppositions. According to our considerations in $KTaO_3$ as temperature decreases to the first transition (*i.e.* over the whole temperature region investigated) in the X-ray pattern all three families of diffuse streaks should be kept (Fig. 1*a*). The direct experimental observation of this in the mono-Laue method would be desirable.

It should be noted that some crystals beyond region (I) on the diagram of perovskite distribution (Fig. 8, part II) but close to the boundary of region (I) may nevertheless be of the shifting type since the radius values may appear to be incorrect and since this very consideration in the assumption of rigid spheres is only an approximation. In particular, this concerns $AgNbO_3$ and $AgTaO_3$ mentioned above. Kania, Roleder & Lukaszewski (1984) and Lukaszewski, Pawelczyk, Handerek & Kania (1983) give some contradictory evidence for a 'tilting' behaviour of these compounds, rather than a 'shifting' behaviour.

Finally, special attention should be paid to some general conclusions which may be drawn from the theory developed. Here it is relevant to refer to a very remarkable discussion in Lines & Glass (1977) on the question of the genuine crystal structure of $BaTiO_3$ type. We can state now that genuine cubic perovskites in the traditional sense do not exist at all. Not a single real perovskite is close-packed in which there are no gaps between ions or not a single perovskite corresponds to point A of Fig. 8 in part II. Hence there are reasons for the existence of movable rigid chains in such crystals (we discuss here only perovskites from the shifting region). Below the first (or sole) phase transition when the chains freeze the crystal structure has the lower symmetry: tetragonal, orthorhombic, rhombohedral. Above this temperature the oscillations of chains take place so that any B atom, for example, does not occupy the centre of the unit cell but with equal probability may be found in eight symmetrical displacements. More precisely if the crystal structure is regarded as that determined *by Bragg scattering only* so a perovskite at $T > T_1$ has cubic symmetry which coincides with that usually described in the literature. But if one determines the crystal structure in a more detailed manner, *i.e.* if the observed *diffuse scattering in addition* is used for the structural analysis so far, a rich picture of the structure will be obtained and no single perovskite is a cubic one.

Remarks on the *A* problem

To obtain Figs. 4 to 9 the mean-field equations with parameters t, l, Δ taken from an intuitive estimation have been calculated. The values of these parameters in rigorous calculations should be obtained with the help of the values for the ionic radii and ionic masses. This is the A problem mentioned above. We shall give only a brief discusssion of it.

Let the first phase transition (from cubic to tetragonal) occur owing to the appearance of spontaneous z shifting. Let us consider the geometrical circumstances before the transition and following the transition and the accompanying reconstruction of the crystal lattice.

The gap between the B and X ions in the earlier (cubic) state is denoted by Δ. Intuitively it is clear that at spontaneous shifting this gap has to lessen and may vanish completely with the opposite displacements of the B and X ions. But, in reality, depending upon the ionic radii and masses, two situations are possible. Either a moving X ion comes in contact with a B ion or it meets side X ions first. Let us denote symbolically these two possibilities by: cubic-$XX(z)$ and cubic-$XB(z)$.

After the spontaneous shifting along the z axis the inevitable lattice contraction in the xy plane takes place owing to the onset of the contraction of the framework of A ions. At this point, X ions in side faces also contract. After such a reconstruction the regime of X-ion motion along the z axis may change. It is easy to understand that the situation cubic-$XX(z)$ may only be strengthened and we shall denote this as tetra-$XX(z)$. As for the cubic-$XB(z)$ contact, this may either be kept [tetra-$XB(z)$] or become tetra-$XX(z)$. Moreover, one should analyse also the motion of the X ions in the transverse direction (along the x axis).

As a result of such an analysis we obtain four possible regimes of z shifting depending upon the ratios of the ionic radii R_X and R_B and their masses M_X and M_B:

Before reconstruction in any x, y or z direction	After reconstruction along z-axis	along x or y axis
(1) cubic-XX	tetra-XX	tetra-XX
(2) cubic-XB	tetra-XX	tetra-XX
(3) cubic-XB	tetra-XB	tetra-XX
(4) cubic-XB	tetra-XB	tetra-XB

After cumbersome calculations one can find the boundaries of all these regimes in two-dimensional space of the variables (r_A, r_B). These boundaries depend also upon the mass ratio $m = M_X/M_B$ as a parameter. Correspondingly one can calculate the t, l and Δ parameters for the mean-field equations in every case.

Omitting the details of the complicated calculations we shall give only a sketch of the subdivision of the shifting region (I) in the diagram (r_A, r_B) into subregions corresponding to these regimes (see Fig. 10). It appears that the numbers of phase transitions in these regimes are different: (1), (2) or (3) transitions of first order and in one case [subregion (1')] only one phase transition of second order. In the latter case the spontaneous shifting causes the decreasing of the amplitudes along the z axis but not the increasing as in the remaining cases.

Considerations of such a kind allow one to understand why in perovskites from the shifting region there may be different numbers of phase transitions. Putting 'the coordinates' (r_A, r_B) of a crystal into the diagram one can predict its behaviour within the framework of the notions 'ionic radii and masses' of course.

Remarks on the order parameter

We denote the oscillation amplitude of the oxygen ion in the cubic phase by Δ_O (Δ_{Nb} for niobium) and the spontaneous displacement (shifting) of the oxygen subchain by $\langle\sigma^z\rangle\Delta_O$ ($\langle\sigma^z\rangle\Delta_{Nb}$ for niobium). In the cubic phase the spontaneous shifting is zero since $\langle\sigma^z\rangle = 0$. Below the transition to the tetragonal phase $\langle\sigma^z\rangle$ appears to be non-zero but the Δ_O (and Δ_{Nb}) value also changes so that both magnitudes $\langle\sigma^z\rangle$ and Δ_O are temperature dependent. The spontaneous shifting of oxygen subchains in the tetragonal phase is $\langle\sigma^z\rangle\Delta_O(\langle\sigma^z\rangle)$. Our task now is to describe the dependence $\Delta_O(\langle\sigma^z\rangle)$. One limiting value at $\langle\sigma^z\rangle \to 0$ is known already; it is Δ_O and can be easily calculated from the geometry of a cell with fixed values of the ionic radii and their masses. In just the same way the amplitude value in the completely formed tetragonal phase, *i.e.* at $\langle\sigma^z\rangle \to 1$, can be calculated. Based on these boundary values we shall approximate $\Delta_O(\langle\sigma^z\rangle)$ by linear dependence: $\Delta_O(\langle\sigma^z\rangle) = \Delta_O(1 + l\langle\sigma^z\rangle)$ and similarly $\Delta_{Nb}(\langle\sigma^z\rangle) = \Delta_{Nb}(1 + l\langle\sigma^z\rangle)$. After such considerations the spontaneous displacements of O subchains and Nb subchains are to be expressed through $\langle\sigma^z\rangle$ only.

Thus although the crystal structure is determined by spontaneous shifting of oxygen and niobium subchains it is determined in reality only by one order parameter, $\langle\sigma^z\rangle$. This is one of the most important advantages of our theory.

At the same time the coupling of the order parameter $\langle\sigma^z\rangle$ with the crystal structure slightly differs from traditional concepts. In fact, although at high temperatures the $\langle\sigma^z\rangle$ value equals zero nevertheless the real perovskite structure is no longer the ideal cubic one. The observation of three families of diffuse-scattering streaks at high temperatures gives rather convincing support to this statement. Quite similarly in the tetragonal phase even at $\langle\sigma^z\rangle \to 1$ the crystal structure is no longer tetragonal but the residual loose packing in the x and z directions (for crystals with two or three transitions) still remains and reveals itself through two families of diffuse streaks in the X-ray pattern.

We have not considered any questions concerning lattice dynamics or any problems in the critical regions such as critical-exponent calculations. The reader may find discussion of such problems in Rytz, Hochli & Bilz (1980), Rytz & Scheel (1982), Fontana, Kugel & Carabatos (1981), Kleemann, Schafer & Fontana (1984), and Kugel, Vogt, Kress & Rytz (1984). We believe that our considerations will help in the understanding of the nature of the mode 'softening' and help to answer the question why any particular mode in a crystal should be a 'soft' one.

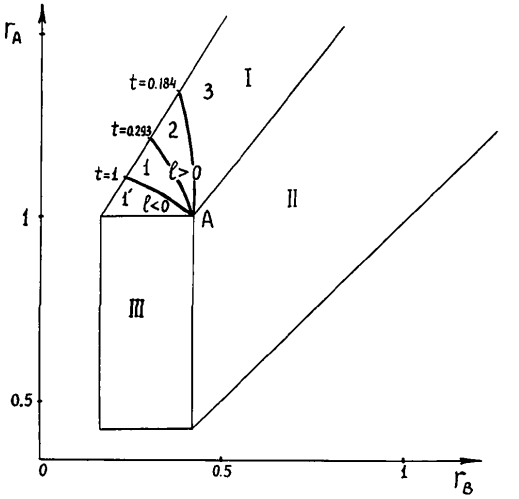

Fig. 10. Subdivision of shifting region (I) into subregions (1'), (1), (2), (3), corresponding to different regimes. Perovskite possesses: one transition of second order, in subregion (1'); one transition of first order, in subregion (1); two transitions of first order, in subregion (2); three transitions of first order, in subregion (3).

References

ALEXANDROV, K. S., ANISTRATOV, A. T., BESNOSIKOV, B. V. & FEDOSEEVA, N. V. (1981). *Phase Transitions in Crystals of Haloid Compounds.* Novosibirsk (USSR): Nauka.

CHRISTENSEN, A. N. & RASMUSSEN, S. E. (1965). *Acta Chem. Scand.* **19**, 421-428.

COMES, R., LAMBERT, M. & GUINIER, A. (1970). *Acta Cryst.* A**26**, 244-254.

FONTANA, M. D., KUGEL, G. E. & CARABATOS, C. (1981). *J. Phys. (Paris) Suppl.* **42**, C6-749-C6-751.

FRANCOMBE, M. H. & LEWIS, B. (1958). *Acta Cryst.* **11**, 175-178.

HARADA, J. & HONJO, G. (1967). *J. Phys. Soc. Jpn*, **22**, 45-57.

JONA, F. & SHIRANE, G. (1962). *Ferroelectric Crystals.* Oxford: Pergamon Press.

KANIA, A., ROLEDER, K. & LUKASZEWSKI, M. (1984). *Ferroelectrics*, **52**, 265-269.

KASSAN-OGLY, F. A. & NAISH, V. E. (1986*a*). *Acta Cryst.* B**42**, 297-306.

KASSAN-OGLY, F. A. & NAISH, V. E. (1986*b*). *Acta Cryst.* B**42**, 307-313.

KAY, H. F. & VOUSDEN, P. (1949). *Philos. Mag.* **40**, 1019-1040.

KLEEMANN, W., SCHAFER, F. J. & FONTANA, M. D. (1984). *Phys. Rev. B*, **30**, 1148-1154.

KUGEL, G. E., VOGT, H., KRESS, W. & RYTZ, D. (1984). *Phys. Rev. B*, **30**, 985-991.

LINES, M. E. & GLASS, A. M. (1977). *Principles and Application of Ferroelectrics and Related Materials.* Oxford: Clarendon Press.

LUKASZEWSKI, M., PAWELCZYK, M., HANDEREK, J. & KANIA, A. (1983). *Phase Transitions*, **3**, 247-258.

MERZ, W. J. (1949). *Phys. Rev.* **76**, 1221-1225.

MERZ, W. J. (1953). *Phys. Rev.* **91**, 513-517.

REMEIKA, J. P. & GLASS, A. M. (1970). *Mater. Res. Bull.* **5**, 37-45.

RYTZ, D., HOCHLI, U. T. & BILZ, H. (1980). *Phys. Rev. B*, **22**, 359-364.

RYTZ, D. & SCHEEL, H. J. (1982). *J. Cryst. Growth*, **59**, 468-484.

TRIEBWASSER, S. (1956). *Phys. Rev.* **101**, 993-997.

TRIEBWASSER, S. (1959). *Phys. Rev.* **114**, 63-70.

Acta Cryst. (1986). B**42**, 325-335

The Immanent Chaotization of Crystal Structures and the Resulting Diffuse Scattering. IV. Diffuse Scattering in Perovskites with Two-Dimensional Movable Objects (Tilting)

BY F. A. KASSAN-OGLY AND V. E. NAISH

Institute of Metal Physics of the Ural Scientific Centre, ul. S. Kovalevskoi 18, *GSP*-170 *Sverdlovsk, USSR*

(*Received* 8 *May* 1985; *accepted* 10 *February* 1986)

Abstract

This paper is devoted to the calculation of the diffuse-scattering picture and its temperature evolution in cubic perovskites, the loose packing of which at high temperatures is connected with the existence of two-dimensional movable objects. The freezing of these objects as temperature decreases leads to structural phase transitions in consecutive order to pseudotetragonal, pseudoorthorhomic and pseudorhombohedral, accompanied by the vanishing of relrod families of diffuse scattering and by the appearence of diffuse (superstructure) reflections. Depending upon the values of the ionic radii crystals with different numbers of phase transitions are possible. The temperature dependence of the order parameters, lattice constants, superstructure reflections, and tilting (antitilting) angles are calculated and compared with experimental data.

Introduction

The present paper immediately follows parts I, II and III (Kassan-Ogly & Naish, 1986*a*, *b*, *c*).

In II we constructed the diagram (Fig. 8 in II) for the existence and stability of ABX_3 compounds based upon the ionic radii, and perovskites were classified as loose-packing types (I), (II) and (III). In the present paper we shall deal with just the perovskites from region (II) of the diagram (tilting).

In such perovskites unit-cell sizes are determined by the contact of B and X ions (Fig. 3 in II). Here B ions are immobile, A ions have three degrees of freedom, and each X ion has two degrees of freedom and, depending on the ionic-radii ratio, is able to meet in its motion either an X ion from the neighbouring cell or A ions from its own cell. This type of loose packing determines, as we shall see later on, the peculiarities of diffuse scattering in perovskites from the tilting region.

The majority of cubic perovskites are found just in this region [see, for example, Alexandrov, Anistratov, Besnosikov & Fedoseeva (1981) and Fesenko (1972)]. However, X-ray patterns in the mono-Laue method have been obtained for only two crystals: $KMnF_3$ (Comes, Denoyer, Deschamps & Lambert, 1971) and $NaNbO_3$ (Denoyer, Comes & Lambert, 1971; Ishida & Honjo, 1973). For only one of these ($NaNbO_3$) has the temperature evolution (although fragmentary) of diffuse scattering been traced, as was done by Comes, Lamber & Guinier (1970) for $KNbO_3$ (a crystal of shifting type). The appearance of three families of

0108-7681/86/040325-11$01.50